Unique chemistry of a diamond-bearing pebble from the Libyan Desert Glass strewnfield, SW Egypt: Evidence for a shocked comet fragment

Article *in* Earth and Planetary Sciences Letters · September 2013

DOI: 10.1016/j.epsl.2013.09.003

CITATIONS
21

READS
433

15 authors, including:

Jan D Kramers
University of Johannesburg
216 PUBLICATIONS **18,902** CITATIONS
SEE PROFILE

Marco Andreoli
University of the Witwatersrand
88 PUBLICATIONS **1,337** CITATIONS
SEE PROFILE

Maria T. Atanasova
Council for Geoscience
12 PUBLICATIONS **104** CITATIONS
SEE PROFILE

Georgy Belyanin
University of Johannesburg
46 PUBLICATIONS **412** CITATIONS
SEE PROFILE

Earth and Planetary Science Letters 382 (2013) 21–31

Contents lists available at ScienceDirect

Earth and Planetary Science Letters

www.elsevier.com/locate/epsl

Unique chemistry of a diamond-bearing pebble from the Libyan Desert Glass strewnfield, SW Egypt: Evidence for a shocked comet fragment

Jan D. Kramers [a,*], Marco A.G. Andreoli [b,c], Maria Atanasova [d], Georgy A. Belyanin [a], David L. Block [e], Chris Franklyn [b], Chris Harris [f], Mpho Lekgoathi [b], Charles S. Montross [g], Tshepo Ntsoane [b], Vittoria Pischedda [h], Patience Segonyane [b], K.S. (Fanus) Viljoen [a], Johan E. Westraadt [g]

[a] Department of Geology, University of Johannesburg, Auckland Park 2006, South Africa
[b] NECSA, PO Box 582, Pretoria 0001, South Africa
[c] School of Geosciences, University of the Witwatersrand, PO Box 3, Wits 2050, South Africa
[d] Council for Geoscience, PO Box 112, Pretoria 0001, South Africa
[e] AECI and AVENG Cosmic Dust Laboratory, School of Computational and Applied Mathematics, University of the Witwatersrand, PO Box 60, Wits 2050, South Africa
[f] Department of Geological Sciences, University of Cape Town, Rondebosch 7701, South Africa
[g] Element Six (Pty) Ltd, Springs 1559, South Africa
[h] LPMCN, Université Lyon 1 and CNRS, UMR 5586, F-69622 Villeurbanne, France

ARTICLE INFO

Article history:
Received 27 November 2012
Received in revised form 27 July 2013
Accepted 3 September 2013
Available online xxxx
Editor: T. Elliot

Keywords:
Libyan Desert Glass
shock diamonds
extraterrestrial carbonaceous matter
carbon isotopes
noble gas isotopes
comet nucleus

ABSTRACT

We have studied a small, very unusual stone, here named "Hypatia", found in the area of southwest Egypt where an extreme surface heating event produced the Libyan Desert Glass 28.5 million years ago. It is angular, black, shiny, extremely hard and intensely fractured. We report on exploratory work including X-ray diffraction, Raman spectroscopy, transmission electron microscopy, scanning electron microscopy with EDS analysis, deuteron nuclear reaction analysis, C-isotope and noble gas analyses. Carbon is the dominant element in Hypatia, with heterogeneous O/C and N/C ratios ranging from 0.3 to 0.5 and from 0.007 to 0.02, respectively. The major cations of silicates add up to less than 5%. The stone consists chiefly of apparently amorphous, but very hard carbonaceous matter, in which patches of sub-μm diamonds occur. $\delta^{13}C$ values (ca. 0‰) exclude an origin from shocked terrestrial coal or any variety of terrestrial diamond. They are also higher than the values for carbonaceous chondrites but fall within the wide range for interplanetary dust particles and comet 81P/Wild2 dust. In step heating, $^{40}Ar/^{36}Ar$ ratios vary from 40 to the air value (298), interpreted as a variable mixture of extraterrestrial and atmospheric Ar. Isotope data of Ne, Kr and Xe reveal the exotic noble gas components *G* and *P3* that are normally hosted in presolar SiC and nanodiamonds, while the most common trapped noble gas component of chondritic meteorites, *Q*, appears to be absent. An origin remote from the asteroid belt can account for these features.

We propose that the Hypatia stone is a remnant of a cometary nucleus fragment that impacted after incorporating gases from the atmosphere. Its co-occurrence with Libyan Desert Glass suggests that this fragment could have been part of a bolide that broke up and exploded in the airburst that formed the Glass. Its extraordinary preservation would be due to its shock-transformation into a weathering-resistant assemblage.

1. Introduction

In an area of about 6000 km^2 in southwest Egypt, close to the border with Libya, fragments of a natural silica-rich glass, known as Libyan Desert Glass (or LDG), of age 28.5 million years, are found (Rocchia et al., 1997; Bigazzi and de Michele, 1996; Horn et al., 1997). These are thought to be the remains of a glassy surface layer, resulting from high temperature melting of sandstones or desert sand, caused either by a meteorite impact (Rocchia et al., 1997), or by an airburst (i.e., a comet exploding in the atmosphere, Seebaugh and Strauss, 1984; Wasson, 2003; Firestone et al., 2007). Platinum-group element abundance patterns (Barrat et al., 1997), osmium isotope data of included dust (Koeberl, 2000), a reduced state of iron-rich portions (Giuli et al., 2003) and graphite-rich bands in the glasses (Pratesi et al., 2002)

* Corresponding author.
E-mail address: jkramers@uj.ac.za (J.D. Kramers).

0012-821X/$ – see front matter
http://dx.doi.org/10.1016/j.epsl.2013.09.003

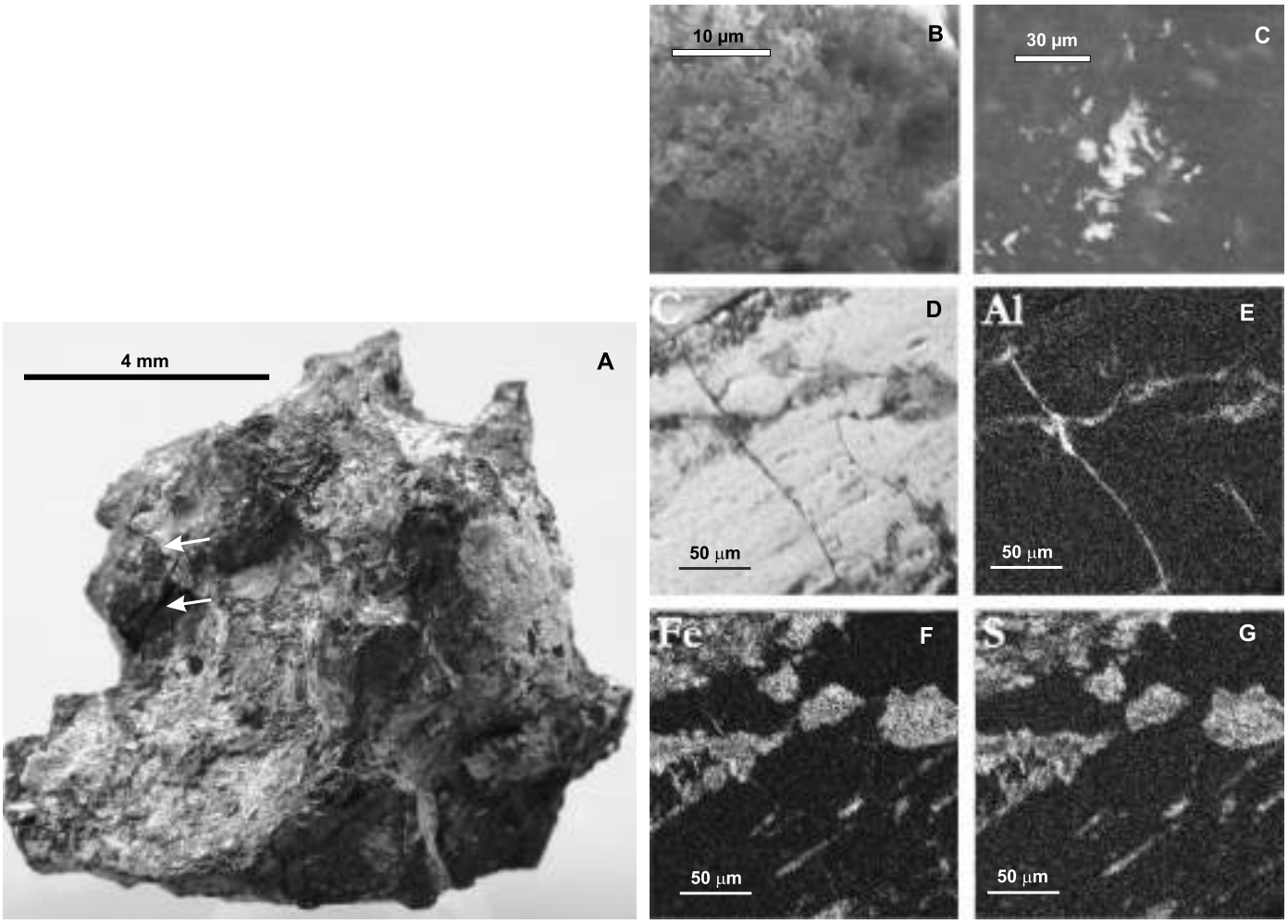

Fig. 1. A: Macrophotograph of sample Hyp-1, the largest among a group of subsamples split from the primary Hypatia stone. Note secondary desert varnish coating and a thin open fracture on the left side (white arrows). **B**, **C**: scanning electron microscope backscattered electron images of a fracture surface on a second subsample (Hyp-2). In **B**, dark material is richer in oxygen than light material. In **C**, light material is Fe–Cr–Ni alloy. Working distance: **B**, 15.1 mm; **C**, 14.4 mm. Detectors: **B**: Everhardt–Thornley; **C**: Dual backscatter. High voltage: **B**, 30 kV; **C**, 20 kV. **D**–**G**: element maps for C, Al, Fe, S (element symbols in left top corners, lighter shades indicate higher concentration) produced on a polished section of Hypatia (Hyp-3) using the TeScan instrument (20 kV). Carbon dominates the matrix (**D**). Aluminum marks secondary clay minerals formed on cracks (**E**). In **F** and **G**, note the close coincidence of Fe with S. Equal abundances signal pyrrhotite.

have been regarded as fingerprints of primitive meteoritic matter. A plausible impact crater 28 km in diameter has been found from Landsat imagery ca. 150 km SW of the center of the LDG strewnfield (Aboud, 2009). However, a crater of that size is unlikely to have significant surface melting associated with it (e.g. Collins et al., 2004).

The stone studied here, approximately 30 g in mass and of dimensions $3.5 \times 3.2 \times 2.1$ cm, was found by Aly A. Barakat in December 1996 at 25°30′E and 25°20′N, in the southwestern part of the LDG field. The locale is in a pebbly corridor situated between the sand dunes of the Wadi Zerzurra area, on sandstone belonging to the Coniacian (88.5–86.6 Ma) Saad Formation (Longinelli et al., 2011). The stone, here named "Hypatia" in honor of the 4th century female philosopher, mathematician and astronomer of Alexandria is uniformly black and shiny with irregular surfaces, some of which are coated with a light brown desert varnish (Fig. 1A). It has a density of ca. 2.2 g/cc, is non-porous, pervasively fractured and very brittle, but has the hardness of diamond in polishing tests. The presence of diamond was confirmed by X-ray diffraction (A.A. Barakat, unpublished Ph.D. Thesis, Cairo University). Thus Hypatia is superficially reminiscent of carbonados. These are black, porous, polycrystalline diamond aggregates of controversial origin (Trueb and de Wys, 1969; Ozima et al., 1991; De et al. 1998, 2001; Garai et al., 2006; Kagi et al., 2007) that have thus far only been found in regions of Brazil and the Central African Republic, where they have been eroded out of Precambrian conglomerates and now occur in alluvial systems.

On the other hand, Hypatia could be connected to the Libyan Desert Glass formation. In this context the stone could be a piece of coal or carbonaceous shale in the target area (Longinelli et al., 2011), shocked into a high pressure phase, as proposed by Barakat (see above), or might be a fragment of a meteorite which impacted, or a shocked remnant of a comet which exploded in our atmosphere. Macroscopic cometary matter has never been found on Earth, and the latter scenario would thus be a unique discovery, opening up a new window on the origin of comets (tens of grams to study in laboratories) and the processes which occur when comets enter planetary atmospheres.

Thus the simple question of Hypatia's origin has important ramifications. To address it, we have carried out exploratory analytical work. Subsamples totaling 1 g available to us were subjected to non-destructive analyses: scanning electron microscopy (SEM), X-ray diffraction (XRD), Raman spectroscopy and deuteron nuclear reaction analysis (NRA). Small quantities were used up in transmission electron microscopy (TEM), C-isotope and noble gas analyses. A comparison of the results with data on relevant terrestrial and

extraterrestrial materials allows the exclusion of the former, and opens an interesting discussion on the latter alternative.

2. Analytical methods

X-Ray Diffraction (XRD) and Deuteron Nuclear Reaction Analysis (D-NRA, for C, O and N) were carried out at the Nuclear Energy Corporation of South Africa (NECSA). NRA is a method well suited to light elements and with a typical depth penetration of 3 μm in solid samples. It was applied to a clean surface (free of secondary crust) using a 4 MV Van de Graaff accelerator. See supplementary text for details, and Supplementary Table 1 for a listing of the nuclear reactions used.

For Scanning Electron Microscopy (SEM) and micro-Raman analysis at the University of Johannesburg (UJ), polishing of a 5×10 mm fragment embedded in epoxy resin was carried out at NECSA and UJ using a Struers MD Piano^{TM} 120 disc which was destroyed in the process.

SEM with Energy Dispersive Spectrometry (EDS) was carried out at NECSA using an FEI Quanta 200 3D instrument on fracture surfaces, and subsequently at UJ with a Tescan Vega3 SEM equipped with an Oxford Instruments XMax 50 mm^2 EDX detector, on a polished surface.

Raman spectroscopy was carried out at NECSA on fracture surfaces using 1064 nm excitation (see supplementary text for details) and subsequently at UJ on a polished surface, using a WiTek Alpha 300R confocal Raman microscope with a frequency-doubled continuous Nd-YAG laser (532 nm) and ca. 5 mW excitation power.

Transmission electron microscopy (TEM) analysis was carried out at Element 6 Ltd. and the Centre of High Resolution TEM at the Nelson Mandela Metropolitan University using a JEOL2100 microscope at 200 kV to image the sample in bright-field and diffraction mode. For sample preparation, a focused Ion Beam SEM (FEI – Helios NanoLab^{TM}) was used. A thin slice (50 nm × 10 μm × 7 μm) was removed from the polished surface of the sample and placed onto a TEM grid for analysis.

The carbon isotope composition of small pieces (1–2 μg) of Hypatia matrix, free of secondary crust, was measured at the Department of Geological Sciences, University of Cape Town, on a Thermo Delta XP Plus mass spectrometer using standard continuous flow methods. See supplementary text for further details.

Noble gas analyses were carried out on five fragments at the University of Johannesburg, using an MAP 215-50 mass spectrometer fitted with a Johnston electron multiplier operated in ion counting mode. Sample preparation was limited to a mild acid leach (10 min cold 0.5 N HNO_3) followed by an acetone wash, each in an ultrasonic bath, to remove surface contaminants.

The grains were stepwise degassed by heating with a defocused beam from a Spectron™ 1064 nm continuous Nd-YAG laser capable of delivering up to 15 W in T_{oo} mode. Heating steps were 5 min except for 10 min for the highest temperature steps. Temperatures, estimated optically and, for the final steps, by visible graphitization, ranged from 600 °C to 1900 °C. As explained in the supplementary text, ^{3}He could not be analyzed, and in the first four analyses (Hyp-7, 9, 10 and 11) $^{40}Ar^{++}$ and CO_2^{++} inhibited ^{20}Ne and ^{22}Ne measurements. This was remedied for fragment Hyp-12.

Calibrations of noble gas abundances and isotope fractionation were based on air volumes from a Dörflinger pipette. Fractionation favors the lighter isotopes and amounts to 1.7%/MU for Ne, 0.9%/MU for Ar, 0.8%/MU for Kr and 0.3%/MU for Xe. Blanks for the full procedure (heating, liquid N_2 trap cooling and heating, and the same time sequence used for the measurements) were reproducible at (cc stp) ^{4}He: $2.6 \pm 0.4 \times 10^{-12}$, ^{21}Ne: $1.2 \pm 0.2 \times 10^{-14}$, ^{36}Ar: $1.2 \pm 0.2 \times 10^{-12}$, ^{84}Kr: $8.6 \pm 1.0 \times 10^{-14}$, ^{132}Xe: $9.3 \pm 1.1 \times 10^{-15}$, for each heating step. Within uncertainty limits, the blanks were of atmospheric composition. All data were corrected for isotope fractionation and (except for Ne) blank abundance and composition.

3. Results and comparisons

3.1. Mineralogy

X-Ray diffraction analysis has shown cubic diamond to be a major phase, while graphite was not detected. Calcite, goethite, quartz, and clay minerals occur as minor phases, probably corresponding to secondary encrustations and fracture fillings.

Scanning electron microscopy of fracture surfaces reveals a texture of two granular, μm-scale phases distinguished by differences in the levels of backscattered electron (BSE-) "grey" (Fig. 1B). Rare, irregularly shaped BSE- "bright" inclusions (up to about 60 μm in length), consisting of a Fe–Cr–Ni alloy were found scattered within the grey matrix (Fig. 1C). Semiquantitative element mapping of a polished surface (Figs. 1D–G) shows dominant carbon, except on fractures where Al indicates clay minerals forming a secondary coating. Patches of high Fe and S (in equal abundance) coincide, indicating pyrrhotite as an important mineral. A detailed study of Hypatia's accessory minerals is currently in progress.

The carbon phases of Hypatia are characterized by Raman spectroscopy. Results from 1064 nm excitation on untreated fracture surfaces (see supplementary text and Supplementary Fig. 1) show that the stone is heterogeneous, with cubic diamond present in some places. The *G* band is broad and centered at a high wave number (1597 cm^{-1}), while graphite would be characterized by a sharp band at 1581 cm^{-1} (Busemann et al., 2007), thus no graphite was detected. A ubiquitous very pronounced background is probably due to the presence of inclusions in the sample (fluorescence) and/or of amorphous matter, which makes quantitative evaluation difficult. In Fig. 2A, a reflected light image of a polished section, the uniform reflectivity and poor polish (due to the extreme hardness) is apparent. In Figs. 2B, C the spectral map and corresponding spectra from micro-Raman mapping with 532 nm excitation of the same polished surface are shown. Diamond appears patchily distributed on a 10 μm-scale within the apparently amorphous matrix. This texture is utterly different from that of carbonados, which are porous aggregates of much coarser diamond grains, without this type of matrix (e.g. De et al., 1998). From comparing Figs. 2B and C, it is also clear that diamond-rich regions do not stand out by being harder than the matrix. Rather, diamond-rich patches appear more pitted. A further remarkable feature of the physical state of Hypatia's matrix is its high thermal stability. Fragments heated up to 1900 °C in vacuum for noble gas extraction showed no change in appearance at all, except for metamorphism and melting of the secondary encrustations and the appearance of minute specs, probably graphite, on the surface at the highest temperatures.

The *D* and *G* bands in the bottom spectrum of Fig. 2C correspond to those shown in Supplementary Fig. 1, obtained by 1064 nm excitation on fracture surfaces. A comparison of Hypatia's non-diamond spectra with the (somewhat similar) *D* and *G* band characteristics of chondritic Insoluble Organic Matter (IOM, Busemann et al., 2007), interplanetary dust particles (IDP's, Busemann et al., 2009) or dust from comet 81P/Wild 2 retrieved by the Nasa's Stardust mission (Rotundi et al., 2008) is rather inconclusive and probably inappropriate, given the great differences in hardness and consistency between the Hypatia matrix and those types of matter.

Fig. 2D shows the nanometer scale texture of a sample, obtained by transmission electron microscopy operating in both the bright field and diffraction mode. Three >100 nm areas of cubic diamond (rich in "dark" specks <10 nm in size where diffrac-

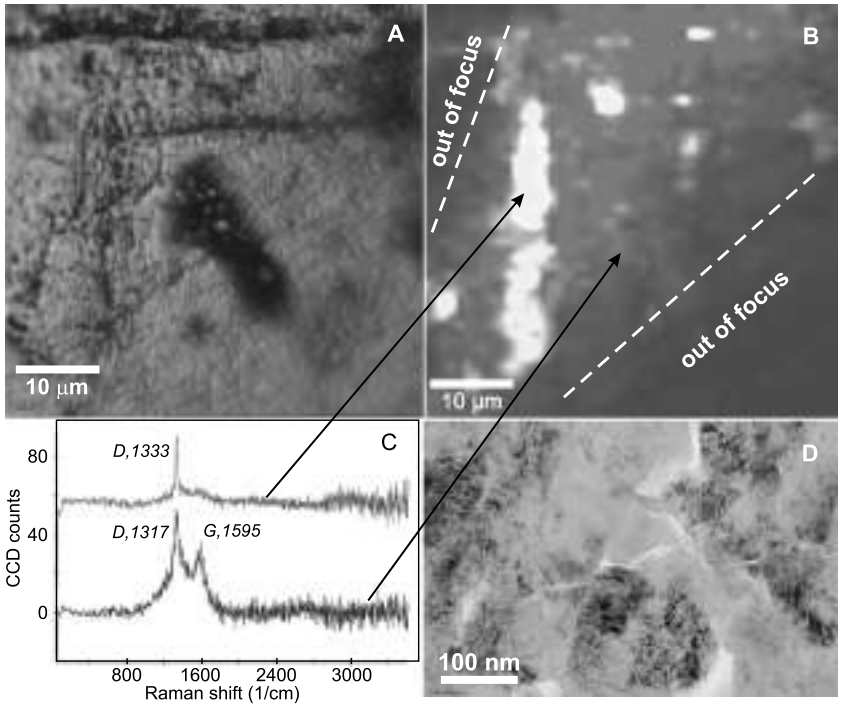

Fig. 2. A: optical image of an area of the polished section of Hyp-3. **B**: Raman spectral map of the same area produced by the WiTek Raman microscope. Light and dark grey patches correspond to the top and bottom spectra shown in **C**, respectively (variable baseline removed). Bottom spectrum in **C** shows both *D* and *G* bands indicating a carbon structure with both sp^2 and sp^3 bonds, whereas in the top spectrum the *G* band is almost absent and the *D* band is very sharp, indicating diamond. Thus light grey areas in **B** are dominated by diamond. **D**: bright-field transmission electron microscope image of a grain from Hyp-3. The nm-scale cracks and voids seen are not an artifact of the sample preparation as they are not observed in similar imagery on terrestrial diamond samples. "Dark" specs are cubic diamond domains with orientations causing electron diffraction. A selected area diffraction pattern of this region (Supplementary Fig. 2) shows several rings, indicating a fine polycrystalline aggregate. A line calibrated profile of the selected area diffraction intensity is shown in Supplementary Fig. 3. Supplementary Table 3 shows the *d*-spacings corresponding to the first 5 rings, and the corresponding diffraction planes in cubic diamond.

tion occurs) are visible (see caption Fig. 2). These diamond areas are much larger than the interstellar (presolar) nanodiamonds (~2 nm, Huss et al., 2003) common in chondritic meteorites, and much smaller than diamonds in ureilitic meteorites (1–10 μm, Jakubowski et al., 2011). They are similar in size to crystallites in polycrystalline diamond aggregates formed by impacts (Koeberl et al., 1997). The specks are mostly elongated and (albeit far less regular) are somewhat reminiscent of planar features in impact-produced diamonds from the Popigai site, interpreted as either nm-scale twinning or stacked defects (Koeberl et al., 1997).

3.2. Bulk chemistry and C-isotopes

In all spots analyzed by EDS and NRA (Table 1) carbon is dominant, while the elements Si, Mg, Al, Fe, Na, Ca, K (the major cation content of silicates) together with Cl and S constitute less than 5% in mass. The high carbon content is reminiscent of terrestrial coal or diamonds, and is much higher than that of any known extraterrestrial material including carbonaceous chondrites, Antarctic micrometeorites (Gounelle et al., 2005), interplanetary dust particles (IDP's, Floss et al., 2006; Matrajt et al., 2012), except cometary matter (Greenberg and Li, 1999) including dust particles from Comet 81P-Wild 2 retrieved by NASA's Stardust mission (Sandford et al., 2006).

The abundance of oxygen is greatly in excess of the cation content, which shows that it is an important element in the carbon dominated matrix. The ranges of O/C and N/C ratios are shown in Fig. 3. There is considerable μm-scale heterogeneity of O/C ratios in Hypatia, which is linked to the mineralogy (see Fig. 1B). The bulk O/C ratios in Hypatia are within the range of coal, significantly higher than values for chondritic IOM, but within the broad range found for comets. Bulk N/C ratios lie within the range for

Table 1
Chemical composition by SEM energy dispersive spectrometry (K emission) and deuteron nuclear reaction analysis C, N, O data on subsample Hyp-3 (see Fig. 1C).

Element	SEM EDS semiquantitive data		Deuteron NRA C, N, O data[b,d]		
	Range (Fig. 1B)[a]	"dark" incl. (Fig. 1C)[a]	Pos 1	Pos 2	Pos 3
C	68–73.3	61.2	76.5	77	74.5
N			1.5	1	0.5
O	19.2–25.0	31.5	22	22	25
Na	0.3–0.8	0.5			
Mg	0.2–0.7	0.4			
Al	0.5–1.9	1.8			
Si	0.7–2.8	3.2			
P	0–0.15	0.03			
S	0–0.5	0.1			
Cl	0–0.5	0.04			
K	0–0.1	0.1			
Ca	0.1–0.6	0.3			
Fe	0.14–1.45	0.75			
N/C			0.0196	0.0130	0.0067
O/C	0.282–0.34	0.51	0.288	0.286	0.335
O/C[c]	0.19–0.34	0.33–0.51			

[a] All data in atomic proportions, in %, not recalculated to 100% total spot.
[b] C, N and O in atomic proportions, summed to 100%.
[c] Possible range of C/O ratios in the C–O–N matrix if some or all of the cations are present as silicates or oxides.
[d] Data for unaltered subsurface material. Reaction product energies listed in Supplementary Table 1 are for particles at the surface of the sample. As the incident beam traverses the sample the ion loses energy, resulting in a lower reaction probability and product energy. Depth profiling was carried out using the SIMNRA fitting procedure (Mayer, 1997). On Hypatia fracture surfaces there is a distinct surface layer about 10^{19} atoms cm^{-1} thick, which has approximately 5× higher N contents than the substrate and this is thought to be due to atmospheric interaction. The nuclear reaction analyses data of C, N and O (atomic proportions summed to 1) listed here reflect the unaltered subsurface material at 3 different locations on the untreated stone surface.

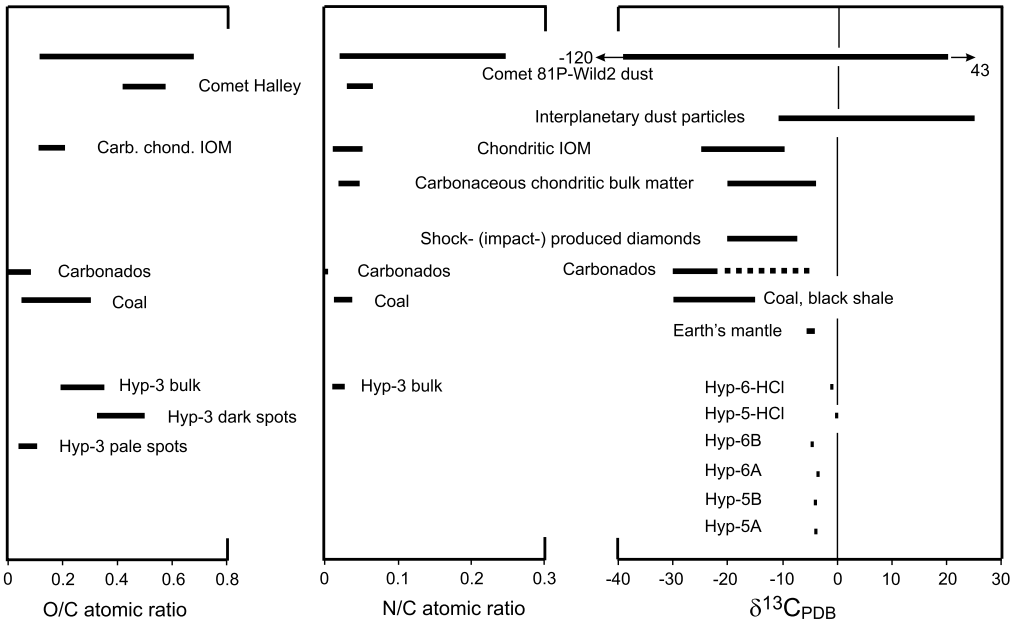

Fig. 3. O/C ratios, N/C ratios (determined both by SEM energy dispersive analysis and nuclear reaction analysis) and $\delta^{13}C_{(PDB)}$ values of Hypatia matrix matter (see Table 1, Supplementary Table 2), compared to terrestrial and extraterrestrial sample sets: coal (Petersen et al., 2008; Ward et al., 2005; Sharp, 2007), bulk carbonaceous chondrites (Kerridge, 1985), chondritic IOM (Alexander et al., 2007), carbonados (De et al., 2001; Kagi et al., 2007; Shelkov et al., 1997), impact-produced diamonds (Koeberl et al., 1997), Comet Halley (Greenberg and Li, 1999), Comet 81P-Wild 2 dust (Sandford et al., 2006; McKeegan et al., 2006; Stadermann et al., 2008; Cody et al., 2008; Matrajt et al., 2008), interplanetary dust particles (Floss et al., 2006; Matrajt et al., 2012), Earth's mantle (Sharp, 2007). All bars include the uncertainty limits. For O/C and N/C ratios of Hypatia, "dark" and "pale" spots refer to Fig. 1B. For $\delta^{13}C$ values, "A" and "B" imply an ultrasonic treatment in ethanol only, whereas "HCl" denotes a cleaning in hot, dilute HCl. Stippled line for carbonados $\delta^{13}C$ represents rare occurrences of heavier values (Shelkov et al., 1997).

coal and at the lower end of the range for chondritic IOM, bulk carbonaceous chondritic matter and comets. Regarding hydrocarbons, the stone appears heterogeneous. Noble gas analyses on fragments Hyp 7, 9, 10 and 11 showed no interfering hydrocarbon masses, but in those on Hyp 12 and other grains surveyed, interferences from hydrocarbons (see supplementary text) impeded Kr and Xe analyses, and large H_2 signals were observed, even up to 1900 °C.

The $\delta^{13}C$ values (see Supplementary Table 2) for variously treated subsamples of the Hypatia matrix are also shown in Fig. 3. Values found after the removal of the desert crusts by ultrasound treatment are reminiscent of terrestrial mantle values. However, after acid treatment, near-zero $\delta^{13}C$ values were obtained, presumably due to removal of remnant secondary carbonate with negative $\delta^{13}C$ values. It is unlikely that significant isotope fractionation occurred in high temperature reactions during putative shock heating (Sharp et al., 2003). However, the values found may not be representative of the material as it existed before a shock event if this was rich in volatiles existing in it as separate phases. A positive correlation between carbon content and $\delta^{13}C$ of bulk carbonaceous chondrites (Kerridge, 1985), and between these and IOM (e.g. Fig. 3) suggests that the more volatile and soluble organic compounds in chondrites have higher $\delta^{13}C$ values than the refractory and insoluble macromolecular matter. The opposite is usually true in terrestrial organogenic matter, where reactions are often biologically mediated (Sharp, 2007). The comparison given in Fig. 3 is nevertheless instructive. It shows a formation from coal or carbonaceous shale to be highly unlikely. Marine carbonates have $\delta^{13}C$ values around zero (Sharp, 2007), but no conversion of these to carbonaceous matter is possible in the atmosphere. The data also indicate a different origin from that of the vast majority of carbonados and terrestrial impact-produced diamonds. Further, the values are well above the ranges associated with typical chondritic IOM and at the upper end of the range for bulk chondrite values. They fall within the (very wide) ranges found for chondritic-porous interplanetary dust particles as well as dust and crater residues

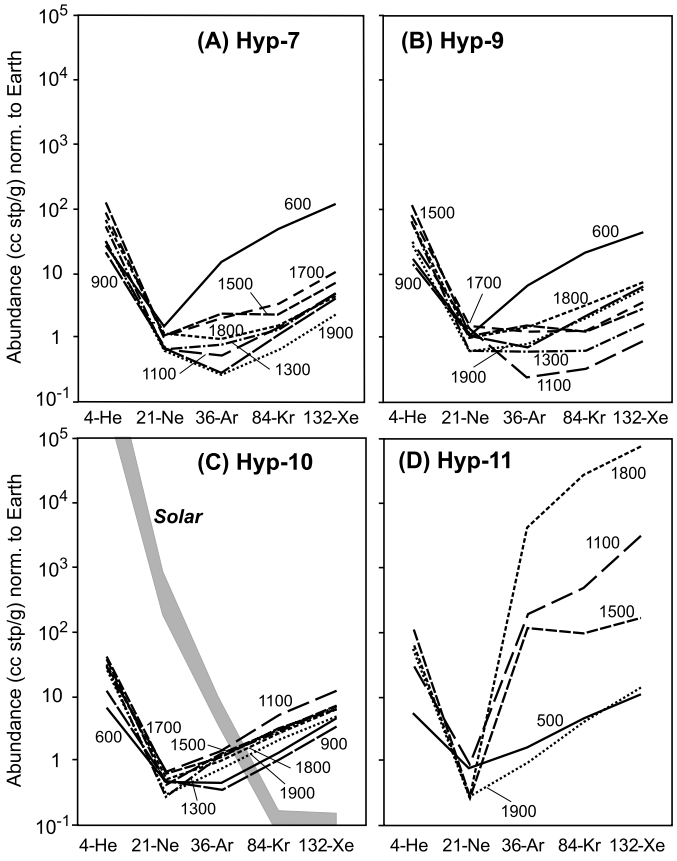

Fig. 4. Noble gas abundances (cc stp/g) for heating steps from Hypatia fragments Hyp-7, -9, -10 and -11, normalized to Earth concentrations (total atmospheric inventory divided by the Earth's mass). Heating step temperatures are shown in °C. For comparison, the atmosphere–normalized *relative* solar abundance pattern (summarized by Wieler, 2002; arbitrarily positioned to fit in the frame) is shown in (C).

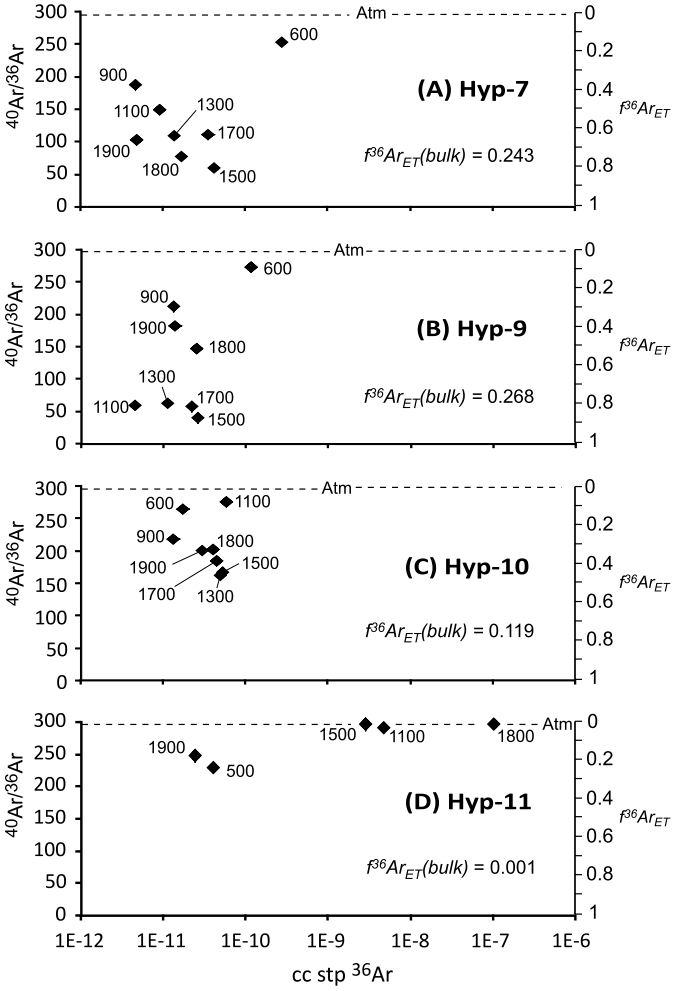

Fig. 5. $^{40}Ar/^{36}Ar$ ratios versus amount of ^{36}Ar released at individual incremental heating steps (temperatures shown in °C). Dashed lines "Atm": Earth's atmosphere. $f^{36}Ar_{ET}$, the extraterrestrial fraction of ^{36}Ar, is scaled on the right hand side of each panel; the bulk value of $f^{36}Ar_{ET}$ listed in the panels is the weighted average of the step values.

sampled in foil from Comet 81P/Wild2 by NASA's Stardust mission.

3.3. Noble gases

Abundances of representative isotopes in cc stp/g for four analyzed fragments are listed in Supplementary Table 4 and plotted in Fig. 4 normalized to the Earth. The U-shaped patterns are at first sight not dissimilar to those in terrestrial sediments (Podosek et al., 1980) where the progressive increase from Ar to Xe reflects greater adsorbtion for the heavy gases. The release patterns of He and Ne appear uniform, and it is remarkable that He was released up to high temperatures even though its thermal diffusivity in mineral matrices is much higher than those of the other noble gases. Ar, Kr and Xe abundances are most variable between steps and fragments. In Hyp-7 and Hyp-9 the first heating step released most of these gases, while in Hyp-10 all steps yielded similar abundances. Hyp-11 stands out by an eruption of gas at 1800 °C that is up to 4 orders of magnitude greater than high-T yields of the other fragments. The noble gases erupted are of atmospheric composition (Fig. 5D, Supplementary Tables 7, 8).

$^{40}Ar/^{36}Ar$ ratios range from 39 to the atmospheric value of 298 (Fig. 5, Supplementary Table 5). These are not analytical artifacts (blank or isobaric interferences) as shown by the following observations: (1) except for some heating steps with very high ^{36}Ar abundance and close to atmospheric Ar, $^{40}Ar/^{36}Ar$ is not correlated with the amount of ^{36}Ar present (Fig. 5); (2), high-resolution scans over ^{36}Ar in the low-abundance steps revealed no interferences for these sample fragments, and (3) the $^{38}Ar/^{36}Ar$ ratios are normal throughout (Supplementary Table 5). Further, a significant cosmic ray produced component of ^{36}Ar (and ^{38}Ar) can be ruled out on the basis of Ne data discussed below. Since no terrestrial reservoirs have $^{40}Ar/^{36}Ar$ ratios below the atmospheric one, an extraterrestrial component is clearly present. All extraterrestrial noble gas species have $^{40}Ar/^{36}Ar < 1$ (Wieler, 2002; Ott, 2002) and if it is assumed that the Ar in Hypatia is a mixture of atmospheric and extraterrestrial Ar, the fraction of extraterrestrial ^{36}Ar, $f^{36}Ar_{ET}$, follows from

$$f^{36}Ar_{ET} = \frac{[(^{40}Ar/^{36}Ar)_{Atm} - (^{40}Ar/^{36}Ar)_{meas}]}{[(^{40}Ar/^{36}Ar)_{Atm} - (^{40}Ar/^{36}Ar)_{ET}]} \quad (1)$$

$f^{36}Ar_{ET}$ is scaled in Figs. 5 A-D, and the bulk value (weighted average) for each fragment is listed. The uncertainties on $^{38}Ar/^{36}Ar$ ratios are too large to distinguish different species of extraterrestrial noble gases, but given the significant fraction of extraterrestrial ^{36}Ar found in fragments Hyp-7, -9 and -10 and a comparison with the solar abundance pattern in Fig. 4C, it is clear that this cannot represent implanted solar wind, as that would have entailed a huge enrichment of Ne and He.

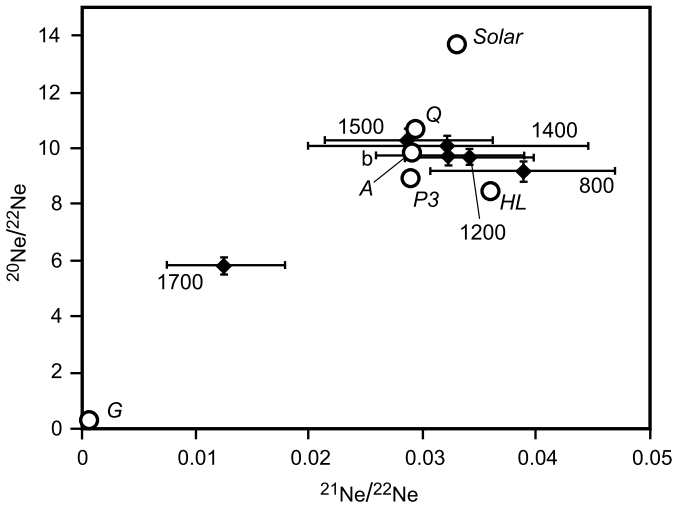

Fig. 6. Conventional three-isotope plot for neon extracted from a large (3.1 mg) fragment (Hyp-12) in broad temperature steps (not corrected for blank (*b*) which is of atmospheric composition; data in Supplementary Table 6), compared with atmospheric (*A*, Pepin and Porcelli, 2002) and the meteoritic trapped components *Q*, *P3*, *HL* and *G* (summarized by Ott, 2002, and discussed in the text). No sample gas from the 1900 °C step could be measured, as a huge eruption of gas occurred (larger than in Hyp-11) which had to be pumped out immediately to prevent damage. A remnant of Ar from this gas, trapped on a cold finger, proved to be of atmospheric composition.

Neon isotope ratios measured on five heating steps of a 3.1 mg fragment, Hyp-12, are listed in Supplementary Table 6 and plotted in Fig. 6 together with the compositions of the blank (b), atmospheric Ne (*A*), solar wind (*Solar*, summarized by Wieler, 2002), and four different components of trapped gases found in meteorites (*Q*, *P3*, *HL* and *G*) that are discussed below. The Ne from four heating steps of Hyp-12 appears dominated by atmosphere (or blank, which is the same) and/or components of similar composition, which cannot be well resolved by the data. The $^{21}Ne/^{22}Ne$ ratios of these four steps are not elevated beyond uncertainties, and thus no cosmogenic ^{21}Ne contribution (by cosmic ray induced reactions on Na, Mg, Al and Si, Niedermann, 2002) is resolvable. Among cosmogenic nuclides, ^{21}Ne has one of the highest production rates. Therefore an effect on the Ar isotope ratios from cos-

mogenic production of ^{38}Ar (from Ca) and ^{36}Ar (from Cl), which have much lower yields, can be ruled out. Further, no implanted solar wind component is apparent. The deviant fifth step (1700 °C) is discussed below.

Trapped noble gas components, summarized by Ott (2002), have distinct ratios of element abundances as well as Ne, Kr and Xe isotopes. The most abundant and ubiquitous is *Q* ("quintessence") gas, also known as *P*1 ("planetary 1") (Lewis et al., 1975; Wieler et al., 1992; Huss et al., 1996; Ozima et al., 1998; Busemann et al., 2000). This appears to be hosted in IOM, is strongly enriched in the heavy noble gases and is mostly regarded as ambient gas of the early solar nebula, possibly derived from the solar noble gas composition by extreme fractionation (Ozima et al., 1998). *P*3, *HL* and *G* are trace components that are mainly hosted in presolar minerals. These have never been analyzed in pure form, and elemental and isotope compositions were derived as end members of mixing arrays. For the purpose of a comparison with Hypatia, three of these are particularly relevant. *P*3 ("planetary 3"; Huss and Lewis, 1994; Huss et al., 2003) is hosted in nanodiamonds and released at temperatures <1000 °C. It is similar to *Q* in its isotope compositions but less enriched in the heavy gases. *HL* ("heavy-light"; Huss and Lewis, 1994; Huss et al., 2003) also occurs in nanodiamonds but is released at temperatures >1000 °C. It is enriched in the heavy and light isotopes of Xe and may be understood as a product of both p- and r-process nucleosynthesis in supernovae. *G* ("giant", also known as S) is hosted in presolar SiC grains and conforms to models of S-process nucleosynthesis in the He-burning shell of Asymptotic Giant Branch (AGB) stars (Gallino et al., 1990; Lewis et al., 1994). *HL* and (particularly) *G* stand out by having Ne, Kr and Xe isotopic compositions very different from *Q* and the Earth's atmosphere, so that small amounts of them can be detected in mixtures. Further minor components (see Ott, 2002) are not relevant for this work.

The only noble gas analysis of cometary matter (Marty et al., 2008) is of Ne and He occurring in very high abundance in (probably metallic) dust particles from Comet 81P/Wild2. Although the Ne isotope ratios are similar to those of *Q* gas, the He has a probably early solar wind implanted component. As there is hardly a basis for comparing these results with those from Hypatia, we focus our comparisons on the chondritic components.

The end member Ne-*G* component consists of almost pure ^{22}Ne (Lewis et al., 1994). In the 1700 °C gas yield of Hyp-12, ^{20}Ne/^{22}Ne and ^{21}Ne/^{22}Ne are both significantly lower than the values for the other steps (Fig. 6), indicating the presence of this component. Analogous to Eq. (1), the amount of $^{22}Ne_G$ from this heating step is calculated to be 42% of total ^{22}Ne.

Krypton and Xe isotope data also yield constraints on the species of extraterrestrial noble gases in Hypatia. At our level of precision, the Kr data (Fig. 7A, Supplementary Table 7) do not allow a distinction between atmospheric Kr or any of the chondritic trapped components except *HL* and *G*. The *G* component has very low ^{83}Kr/^{84}Kr and enhanced ^{82}Kr/^{84}Kr ratios compared to other Kr species (Lewis et al., 1994; Ott, 2002). ^{86}Kr/^{84}Kr ratios of *G* are also anomalously high, but highly variable and unsuitable for quantitative assessments. In a plot of ^{83}Kr/^{84}Kr vs. ^{82}Kr/^{84}Kr (Fig. 7A) a tail from the "common" (atmospheric, solar wind, *Q* and *P*3) isotope compositions towards lower ^{83}Kr/^{84}Kr and higher ^{82}Kr/^{84}Kr is visible. Fractionation trends shown in Fig. 7A run at right angles to this tail, indicating that it cannot be an artifact of fractionation during degassing. The 95% confidence envelope of a York fit through the data (Ludwig, 2000) includes the remote *G* composition. No significant *HL* contribution is indicated.

If it is assumed that the data array portrays a binary mixture between "common" and *G*, the fraction of $^{84}Kr_G$ ($f^{84}Kr_G$) in the mixture is derived in a way analogous to $f^{36}Ar_{ET}$ above (Eq. (1)), with the benefit of two mixing arrays, so that the average of two results can be used. Given the large uncertainties of individual data points, the $f^{84}Kr_G$ values for the bulk fragments Hyp-7, Hyp-9 and Hyp-10 are surprisingly consistent between 0.026 and 0.027 (Table 2A; Hyp-11 is not included as it is fully dominated by atmospheric Kr). The 95% confidence limits (obtained by a Monte Carlo approach) for the individual fragments and for the composite of all three fragments are small compared to the values, thus the results are significant, demonstrating the presence of a *G* component, in accord with the Ne data from the 1700 °C step of Hyp-12 (Fig. 6).

The Xe isotope data (Figs. 7 B, C, Supplementary Table 8) are in stark contrast to those obtained by Ozima et al. (1991) on carbonados, which showed a large fissiogenic component. Instead, it is possible to discern a mixture of a dominant terrestrial atmospheric component and extraterrestrial Xe. Atmospheric Xe is strongly fractionated relative to common extraterrestrial gases, with a depletion of the lighter isotopes (e.g. Pepin and Porcelli, 2002). The ^{128}Xe/^{132}Xe ratio shows the strongest effect (15%) and in Fig. 7B this is plotted against ^{136}Xe/^{132}Xe, which allows a differentiation between different ET components. In spite of the large individual error limits, the 95% confidence envelope of regression of all data allows to exclude *HL* as a significant components, and also confirms the exclusion of a major implanted solar wind contribution as also inferred from the element abundance patterns (Fig. 4) and Ne isotopes (Fig. 6). The swathe includes the *Q* and *P*3 compositions, barely misses the remote *G* composition indicated as a component by the Kr data, but also includes the fractionation trend. In the plot of ^{129}Xe/^{132}Xe vs. ^{136}Xe/^{132}Xe ratios (Fig. 7C), however, the fractionation trend is at a high angle to the data array, indicating that the variations seen in both Figs. 7 B and C do not result from mass fractionation. Fig. 7C allows a further resolution of the ET components, thanks to the strong depletion of ^{129}Xe in *G* (Lewis et al., 1994; Gallino et al., 1990). Now the data portray a three-component mixture of atmospheric, *Q* and/or *P*3, and minor *G*.

A three-component mixture (*mix*) with two isotope ratio ranges can be taken apart if the isotope ratios of the end members are known. If *T* and *U* denote ^{129}Xe/^{132}Xe and ^{136}Xe/^{132}Xe, respectively, the components are *A* (atmosphere), *P* (for *Q* and/or *P*3) and *G* and $f_A + f_P + f_G = 1$, then $f_A T_A + f_P T_P + f_G T_G = T_{mix}$, and analogous for *U*, giving three linear equations. Substitution and rearranging yields:

$$f_G = \frac{[(U_P - U_A)(T_{mix} - T_A) - (T_P - T_A)(U_{mix} - U_A)]}{[(U_P - U_A)(T_G - T_A) - (U_G - U_A)(T_P - T_A)]} \quad (2)$$

and similar for f_P, or f_A, yielding the three fractions. The results for the fractions f_G and f_P (summed over all steps of each fragment) are listed in Table 2A for fragments Hyp-7, Hyp-9 and Hyp-10 (Hyp-11 is fully dominated by atmospheric Xe, as for Kr). For Hyp-9 and Hyp-10 the 95% confidence limits (obtained by a Monte Carlo approach) are larger than the values. However, the f_G and f_P values show reasonable consistency and for Hyp-7 and the composite the 95% confidence limits are smaller than the values (Table 2A). f_G and f_P are thus significantly above zero, confirming the visual impression of Fig. 7B indicating the three components.

The various types of chondritic noble gases have different abundance ranges and very distinct inter-element ratios, which also provide a basis for a tentative comparison with the ET components of Hypatia (Table 2B, C). While the total ET fraction of ^{84}Kr in Hypatia is unknown, the abundances of $^{84}Kr_G$, $^{132}Xe_G$ and $^{132}Xe_{P3,\,Q}$ are constrained. Further, the ^{36}Ar/^{132}Xe ratio of *G* gas is very small compared to that in the *Q* or *P*3 gases (Table 2C), so that the ET fraction of ^{36}Ar in the Hypatia fragments must belong to *P*3 and/or *Q*. Therefore $(^{36}Ar/^{132}Xe)_{P3,\,Q}$ is also constrained. In addition, we think the ^{4}He content found is essentially extraterrestrial, because He is a non-sorbent, low-abundance gas in the atmosphere, and from its uniform abundance in the fragments and

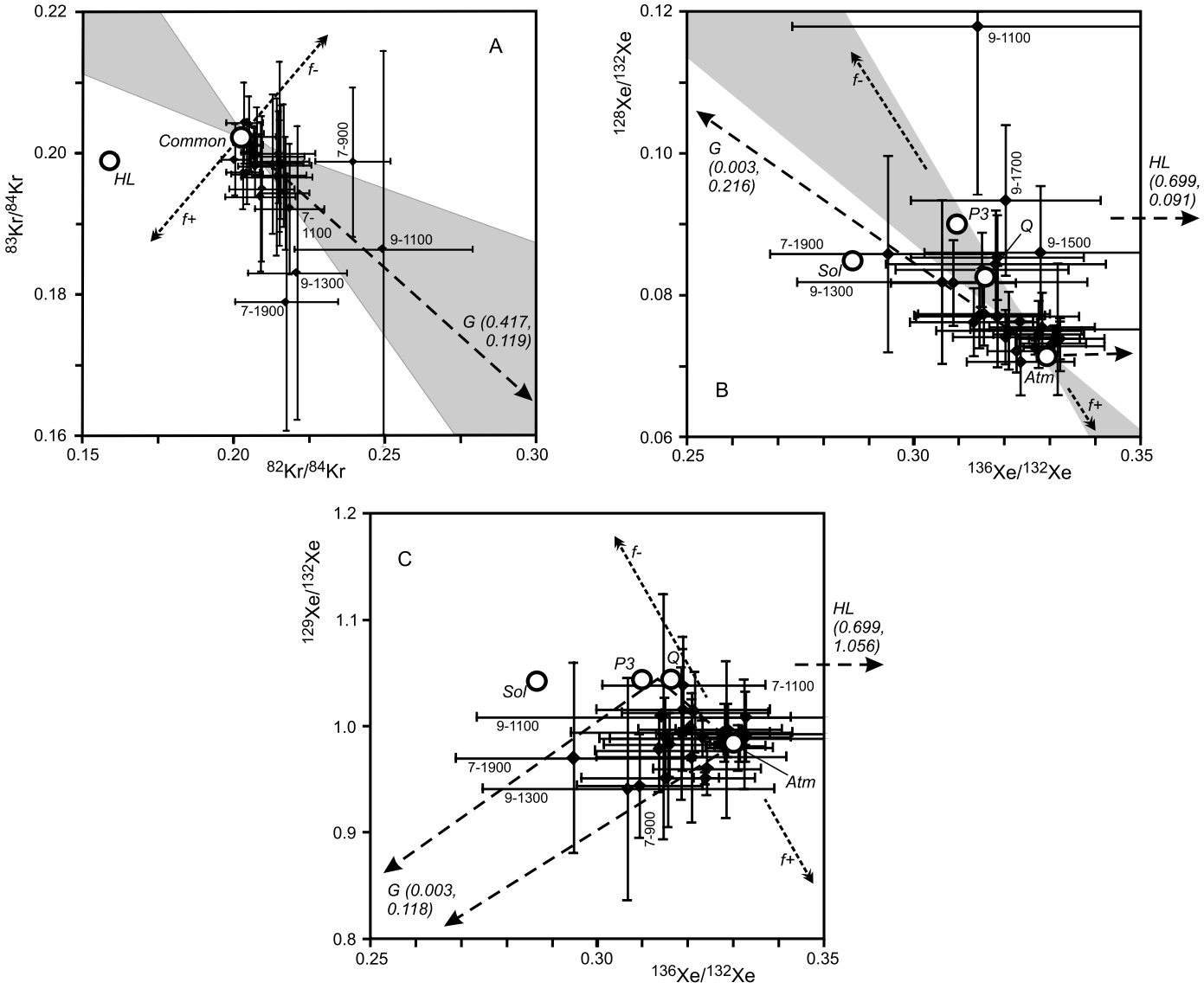

Fig. 7. Three-isotope plots for Kr and Xe from the heating steps of four Hypatia fragments, shown with 2σ error bars, compared with atmospheric and various extraterrestrial isotope compositions. Narrow-dashed arrows with double heads show direction of mass-dependent fractionation enriching heavy ($f+$) or light ($f-$) isotopes. Labels on data points deviating strongly from the main populations give the Hyp-number and the step temperature in °C (referring to Supplementary Tables 7 and 8). **A**: Krypton data. "Common" comprises isotopic compositions of atmospheric, solar wind, *Q* and *P*3 components discussed in the text, as summarized by Ott (2002), Wieler (2002) and Pepin and Porcelli (2002), which are not resolved at this scale. Only the *HL* and *G* components are clearly different. Broad-dashed arrow points to *G* composition outside the plot. Grey area is 95% confidence envelope of a York fit through the Hypatia data only (not forced through "common"). **B**: $^{128}Xe/^{132}Xe$ vs. $^{136}Xe/^{132}Xe$, *Atm*: atmosphere (Pepin and Porcelli, 2002), *Sol*: solar wind (Wieler, 2002). Isotopic compositions of chondritic noble gas components as for **A**. Broad-dashed arrows with coordinates point to the components outside the plot. Grey area as in **A**. **C**: $^{129}Xe/^{132}Xe$ vs. $^{136}Xe/^{132}Xe$. The dashed triangle (apices *Atm*, *Q* and arrows pointing to distant *G* component) contains most of the data, suggesting 3-component mixing as discussed in the text.

release up to high temperature steps it appears unlikely that it originated as α-particles from the decay of U introduced in the weathering environment. Owing to the vast differences in abundances and inter-element ratios between the chondritic noble gas components, it is valid to make comparisons between them and the Hypatia data in spite of the large uncertainties.

The $^{84}Kr_G$ abundance in Hypatia is about 2 orders of magnitude higher than in bulk chondrites, while that of $^{132}Xe_G$ overlaps with the top of the chondritic range. Thus the $(^{84}Kr/^{132}Xe)_G$ ratio of Hypatia is 1 to 2 orders of magnitude higher than the range found for this ratio by Lewis et al. (1994) in SiC grains of the Murchison meteorite. These authors note, however, that $(^{84}Kr/^{132}Xe)_G$ in SiC is highly variable, correlated with grain size, and about an order of magnitude lower than predicted by modeling of the S-process in AGB stars (Gallino et al., 1990). The $(^{84}Kr/^{132}Xe)_G$ ratio of Hypatia is therefore not implausible.

The $(^{36}Ar/^{132}Xe)_{P3,\,Q}$ ratios for bulk fragments Hyp-7, Hyp-10 and the composite of all three are significantly higher than those of *Q*-gas, and similar to *P*3. Also, from the composite of the three fragments, the $^{4}He/^{132}Xe_{P3,\,Q}$ ratios are resolvably an order of magnitude higher than in *Q*, but lower than in *P*3. Admixture of *G* gas would raise the $^{4}He/^{132}Xe$ ratios further (Table 2C). No single known component fits fully to the inter-element ratio constraints, but if it is accepted that Hypatia might have lost He in its history (compare the extreme He-depletion in ureilites, which have undergone shock, Ott, 2002; Rubin, 2006) then the extraterrestrial non-*G* component in Hypatia appears more similar to *P*3 than to *Q*.

The abundances of *Q*-Xe and *P*3-Xe are highly variable in chondrites and both are found to decrease with progressive thermal processing (Huss et al. 1996, 2003). The ranges are given in Table 2C, and it can be seen that the abundance of $^{132}Xe_{P3,\,Q}$ in

Table 2
Extraterrestrial components of noble gases in Hypatia.

A. Total gas amounts (cc stp) and extraterrestrial fractions

Fragment	Mass (g)	^{4}He $\times10^{-9}$	^{36}Ar $\times10^{-10}$	^{84}Kr $\times10^{-11}$	^{132}Xe $\times10^{-12}$	$f^{36}Ar_{ET}$ ±95%	$f^{84}Kr_{G}$ ±95%	$f^{132}Xe_{G}$ ±95%	$f^{132}Xe_{Q,P3}$ ±95%
Hyp-7	0.00085	1.29	4.06	2.28	2.23	0.320 ± 0.010	0.0265 ± 0.0144	0.0056 ± 0.0053	0.156 ± 0.091
Hyp-9	0.00082	1.22	2.38	1.18	0.967	0.365 ± 0.011	0.0267 ± 0.0139	0.0084 ± 0.0099	0.079 ± 0.153
Hyp-10	0.00190	1.53	3.15	1.83	1.65	0.313 ± 0.009	0.026 ± 0.0109	0.0033 ± 0.0078	0.136 ± 0.127
Composite	0.00357	4.03	9.59	5.29	4.84	0.329 ± 0.007	0.0264 ± 0.0077	0.0054 ± 0.0042	0.134 ± 0.068

B. Absolute abundances of extraterrestrial components (cc stp/g) and interelement abundance ratios

Fragment	$^{4}He_{Q,P3,G}$ $\times10^{-7}$	$^{36}Ar_{Q,P3}$ $\times10^{-8}$	$^{84}Kr_{G}$ $\times10^{-10}$	$^{132}Xe_{G}$ $\times10^{-12}$	$^{132}Xe_{P3,Q}$ $\times10^{-10}$	$^{4}He/^{132}Xe_{Q,P3}$ ±95%	$(^{36}Ar/^{132}Xe)_{Q,P3}$ ±95%	$(^{84}Kr/^{132}Xe)_{G}$ ±95%
Hyp-7	15 ± 3	15 ± 1.6	7.1 ± 3.9	15 ± 14	4.1 ± 2.4	3575 ± 2275	375 ± 225	49 ± 53
Hyp-9	15 ± 3	11 ± 1.1	3.8 ± 2.0	9.9 ± 12	0.93 ± 1.8	14461 ± 27147	1137 ± 2208	39 ± 50
Hyp-10	8 ± 1.6	5.2 ± 0.54	2.5 ± 1.0	2.9 ± 6.8	1.2 ± 1.1	6631 ± 6587	438 ± 414	87 ± 209
Composite	11 ± 1.1	8.8 ± 0.52	3.9 ± 1.2	7.3 ± 5.7	1.8 ± 0.94	5973 ± 3207	486 ± 253	53 ± 45

C. Comparisons with carbonaceous chondritic matter

Gas type	^{84}Kr	^{132}Xe	$^{4}He/^{132}Xe$	$^{36}Ar/^{132}Xe$	$^{84}Kr/^{132}Xe$
	cc stp/g in bulk chondrite				
Q (Huss et al., 1996; Busemann et al., 2000)		$(5–80) \times 10^{-10}$	374 ± 72	45–110	0.5–1.2
*P*3 (Huss and Lewis, 1994; Huss et al., 2003)		$(0.01–15) \times 10^{-10}$	$(6.7 \pm 2.0) \times 10^{4}$	400 ± 25	2.7 ± 0.4
G (Lewis et al., 1994)	$(0.3–1.5) \times 10^{-12}$	$(0.1–8) \times 10^{-12}$	$(32 \pm 5) \times 10^{4}$	3.5 ± 0.5	0.2–7.5

Hypatia is close to the lower end of the range for $^{132}Xe_{Q}$ in bulk chondrites, and is in the upper part of their $^{132}Xe_{P3}$ range. The ratio $^{132}Xe_{G}/^{132}Xe_{P3,Q}$ in Hypatia is between 0.03 and 0.1, which is at least 30× higher than $^{132}Xe_{G}/^{132}Xe_{Q}$ of chondrites, but well within their range for $^{132}Xe_{G}/^{132}Xe_{P3}$. These data are all in accord with the dominant ET Xe component in Hypatia being mostly (or all) *P*3, rather than *Q*.

Another surprising feature of Hypatia is the lack of a detectable *HL* component (Figs. 6, 7). In chondrites the *HL*-Xe component is approximately equal in abundance to *P*3-Xe (Huss et al., 2003). If that were the case in Hypatia, *HL*-Xe should have been clearly detectable given its highly anomalous isotope composition, but it is not seen. Summarizing, the inventory of ET noble gases in Hypatia, inasmuch as our exploratory data allow it to be defined, differs from that of bulk chondrites in the apparent absence of the *Q* and *HL* components, and an overabundance of *G*-Kr.

4. Discussion

The clearest indication of an extraterrestrial origin of at least part of Hypatia is given by the Ar isotope data. Further, the $\delta^{13}C$ values exclude terrestrial carbonaceous matter. Together, these data amount to evidence that Hypatia is an extraterrestrial object. Before speculations are made about what type of matter it represents, the questions of its very unusual mineralogy, and why it contains such a large, heterogeneously distributed abundance of atmospheric noble gases, must be addressed.

Diamond is patchily distributed, the grains appear disrupted and are most similar (or least dissimilar) to impact-related diamonds. It is most likely that they have been generated in a pressure shock. In principle such a shock could have been associated with Hypatia's encounter with the Earth, or with an earlier, extraterrestrial impact as is the case in ureilites (Rubin, 2006). However, the high abundance of atmospheric noble gases in Hypatia, released up to high temperature steps, indicates that the final event shaping the present state of the stone occurred in the Earth's atmosphere. The atmospheric gas eruptions from fragments Hyp-11 and -12 at 1800 °C in particular suggest that inclusions of highly compressed atmosphere are present. The amount of ^{36}Ar released from Hyp-11 at 1800 °C would correspond to 0.027 cc stp of total argon, or 2.7 cc stp of bulk atmosphere, whereas the volume of fragment Hyp-11 is ca. 0.001 cc.

Large aerial bursts occur when mechanically weak bolides break up into many smaller fragments prior to impact, so that a large portion of their kinetic energy goes towards heating the atmosphere (Wasson, 2003). This can produce surface melt sheets such as documented by the LDG. Airbursts in themselves are not predicted to generate high pressures, but large airbursts and Earth surface impacts of fragments can occur in the same event, as is demonstrated by the presence of coesite in some glasses (Wasson, 2003). Diamonds can indeed form very rapidly in shock events. However in all studied cases graphite is present as a precursor (Kenkmann et al., 2005; Koeberl et al., 1997) and the apparent absence of graphite in Hypatia thus presents a problem in this context, which has to be addressed in more detailed mineralogical work. Nevertheless the suggestion that Hypatia represents part of an impacted fragment of an object that also generated an airburst is tempting, as this scenario could account for the diamondiferous mineralogy, the presence of atmospheric noble gases and the LDG itself.

Any consideration of the original nature of Hypatia must take into account its chemistry and the unusual apparent composition of its extraterrestrial noble gas component. A continuum in compositions between CI chondrites and comets has been suggested (Lodders and Osborne, 1999; Gounelle et al., 2005, 2006; Aléon et al., 2009), but C contents as high as that of Hypatia are only seen in dust from Comets Halley and 81P/Wild2 (Jessberger, 1999; Sandford et al., 2006), some interplanetary dust particles (Floss et al., 2006; Matrajt et al., 2012) and micrometeorites recovered from Antarctic ice considered to be of cometary origin (Duprat et al., 2010).

The noble gas content of Hypatia does not offer a direct comparison with cometary matter, but nevertheless yields clues on the stone's origin. In the extraterrestrial component, the apparent lack of *Q* and *HL* gases is striking. It is unlikely that this is due to impact effects, as an important atmospheric component, presumably picked up immediately before impact, was retained. Also, the *P*3 noble gas component is normally considered "labile", being released from chondritic matter below 1000 °C in step heating analyses, whereas *HL* appears in high temperature fractions (Huss et al., 2003). In Hypatia, *P*3 and *G* were released together up to high temperatures, and this suggests that the *P*3 host is encapsulated in the shock-transformed matrix. This should then apply to *Q* as well, if it were present. The absence of *Q* and *HL* gases in

Hypatia is thus a further clear difference between the stone and chondrites, in which these gases are ubiquitous.

The *Q* component in chondrites is mostly considered to represent the ambient gas of the early solar nebula in the region where the primitive asteroids agglomerated, and adsorbed it (Huss et al., 1996; Ozima et al., 1998; Ott, 2002). In this context, the absence of *Q* gas in Hypatia could therefore indicate that there were no ambient heavy noble gases present in the region where its matrix formed. Following three solar nebula models, temperatures during early accretion in the outer nebula (between 30 and 50 AU from the sun, in the present Kuiper Belt) were below 70 K, and pressures below 10^{-8} bar (Fegley, 1999). Under these conditions there would be a very little Ar, Kr or Xe present in gaseous form to be adsorbed. The *HL* (supernova) gas component is hosted in a different nanodiamond population from *P*3 (Ott, 2002). Its absence in Hypatia could imply that this particular population was heterogeneously distributed in the solar nebula, and that it did not occur is the region where the impactor agglomerated. The notion that Hypatia's region of origin was far from the asteroid belt, probably in the Kuiper Belt, could thus account for the absence of both *Q* and *HL* gases in the stone.

From the size of an object required to generate shock diamonds it can be concluded that there should be many more fragments similar to the Hypatia stone near the impact site. The hypothesis of a connection with the 28.5 Ma LDG event implies a remarkable resistance to weathering for the stone. Therefore large quantities of (albeit shocked) cometary matter might be found in the area around the Hypatia find, enabling the future study of many aspects of the outermost solar system.

5. Summary and conclusions

Our exploratory work on Hypatia has established the following results beyond doubt: first, the stone is of extraterrestrial origin (from Ar isotopes and δ^{13}C values); second, carbon is its dominant constituent and O/C ratios are higher than those of chondritic IOM, but the combined content of cations that make up silicates is less than 5%; third, in its Ar and Xe (and probably also Kr) content an atmospheric component is dominant. In a hypothesis that can account for these data, the following scenario is proposed: An object similar in composition to cometary nuclei entered the Earth's atmosphere, where it lost volatile hydrocarbons and ices, and adsorbed heavy noble gases before impacting with sufficient velocity to generate shock diamonds. It is surmised that this object was a fragment of the larger bolide that generated the airburst responsible for the formation of the Libyan Desert Glass. Its preservation is ascribed to the shock transformation of its matrix.

From isotope compositions of Ne, Kr and Xe and element ratios it is further inferred that Hypatia's extraterrestrial noble gas content consists essentially of two components: *P*3, which in chondrites is hosted in nanodiamonds, and *G*, normally hosted in presolar SiC grains. Two components that are ubiquitous in chondrites *Q* and *HL*, are inferred to be absent. These observations strengthen the hypothesis that the impactor did not originate from the asteroid belt. It was probably formed in a more external region of the solar nebula, such as the Kuiper Belt.

Acknowledgements

We thank Aly A. Barakat (Egyptian Geological Survey and Mining Authority), Mario di Martino (INAF-Astrophysical Observatory of Torino), Vincenzo de Michele (formerly Natural History Museum, Milano), Romano Serra (Physics Department, Bologna University) and Gawie Nothnagel (Necsa) for samples and valuable discussions, Roberto Appiani (gmlmilano@libero.it) for Hypatia's macrophotograph, Michael Witcomb (UW) for SEM EDS analyses, Ian Newton (Dept. of Archaeology, UCT) for assistance with the C-isotope analyses, Jan-Maarten Huizenga (North West University) for the diamond standard, and the Centre of High Resolution TEM at the Nelson Mandela Metropolitan University for use of their FIB – SEM and JEOL2100 TEM. De Beers Geoscience generously donated the noble gas laboratory at UJ. The Cosmic Dust Laboratory at the University of the Witwatersrand is sponsored by AECI and AVENG. The highly relevant comments by Rainer Wieler and two anonymous reviewers have led to considerable improvements in the manuscript.

Appendix A. Supplementary material

Supplementary material related to this article can be found online at http://dx.doi.org/10.1016/j.epsl.2013.09.003.

References

Aboud, T., 2009. Libyan Desert Glass: has the enigma of its origin been resolved? Phys. Proc. 2, 1425–1432.

Aléon, J., Engrand, C., Leshin, L.A., McKeegan, K.D., 2009. Oxygen isotopic composition of chondritic interplanetary dust particles: A genetic link between carbonaceous chondrites and comets. Geochim. Cosmochim. Acta 73, 4558–4574.

Alexander, C.M., Fogel, M., Yabuta, H., Cody, G.D., 2007. The origin and evolution of chondrites recorded in the elemental and isotopic compositions of their macromolecular organic matter. Geochim. Cosmochim. Acta 71, 4380–4403.

Barrat, J.A., et al., 1997. Geochemistry and origin of Libyan Desert Glasses. Geochim. Cosmochim. Acta 61, 1953–1959.

Bigazzi, G., de Michele, V., 1996. New fission-track age determination on impact glasses. Meteorit. Planet. Sci. 31, 234–236.

Busemann, H., et al., 2009. Ultra-primitive interplanetary dust particles from the comet 26P/Grigg–Skjellerup dust stream collection. Earth Planet. Sci. Lett. 288, 44–57.

Busemann, H., Alexander, C.M.O.D., Nittler, L.R., 2007. Characterization of insoluble organic matter in primitive meteorites by micro Raman spectroscopy. Meteorit. Planet. Sci. 42 (1387–1416).

Busemann, H., Baur, H., Wieler, R., 2000. Primordial noble gases in "phase Q" in carbonaceous and ordinary chondrites studied by closed-system stepped etching. Meteorit. Planet. Sci. 35, 949–973.

Cody, G.D., et al., 2008. Quantitative organic and light-element analysis of comet 81P/Wild 2 particles using C-, N-, and O-μ-XANES. Meteorit. Planet. Sci. 43, 353–365.

Collins, G.S., Melosh, H.J., Ivanov, B.A., 2004. Modeling damage and deformation in impact simulations. Meteorit. Planet. Sci. 39, 217–231.

De, S., Heaney, P.J., Hargraves, R.B., Vicenzi, E.P., Taylor, P.T., 1998. Microstructural observation of polycrystalline diamond: A contribution to the carbonado conundrum. Earth Planet. Sci. Lett. 164, 421–433.

De, S., Heaney, P.J., Vicenzi, E.P., Wang, J., 2001. Chemical heterogeneity in carbonado, an enigmatic polycrystalline diamond. Earth Planet. Sci. Lett. 185, 315–330.

Duprat, J., et al., 2010. Extreme deuterium excesses in ultracarbonaceous micrometeorites from central Antarctic snow. Science 328, 742–745.

Fegley Jr., B., 1999. Chemical and physical processing of presolar materials in the solar nebula and the implications for preservation of presolar materials in comets. Space Sci. Rev. 90, 239–252.

Firestone, R.B., West, A., Kennett, J.P., Becker, L., et al., 2007. Evidence for an extraterrestrial impact 12,900 years ago that contributed to the megafaunal extinctions and the Younger Dryas cooling. Proc. Natl. Acad. Sci. USA 104, 16016–16021.

Floss, C., et al., 2006. Identification of isotopically primitive interplanetary dust particles: A NanoSIMS isotopic imaging study. Geochim. Cosmochim. Acta 70, 2371–2399.

Gallino, R., Busso, M., Picchio, G., Raiteri, G.M., 1990. On the astrophysical interpretation of isotope anomalies in meteoritic SiC grains. Nature 348, 298–302.

Garai, J., Haggerty, S.E., Rekhi, S., Chance, M., 2006. Infrared absorption investigations confirm the extraterrestrial origin of carbonado diamonds. Astrophys. J. 653, L153–L156.

Giuli, G., Paris, E., Pratesi, G., Koeberl, C., Cipriani, C., 2003. Iron oxidation state in the Fe-rich layer and silica matrix of Libyan Desert Glass; a high-resolution XANES study. Meteorit. Planet. Sci. 38, 1181–1186.

Gounelle, M., et al., 2005. Small Antarctic micrometeorites: A mineralogical and in situ oxygen isotope study. Meteorit. Planet. Sci. 40 (6), 917–932.

Gounelle, M., Spurný, P., Bland, P.A., 2006. The orbit and atmospheric trajectory of the Orgueil meteorite from historical records. Meteorit. Planet. Sci. 41 (1), 135–150.

Greenberg, J.M., Li, A., 1999. Morphological structure and chemical composition of cometary nuclei and dust. Space Sci. Rev. 90, 149–161.

Horn, P., Müller-Sohnius, D., Schaaf, P., Kleinmann, B., Storzer, D., 1997. Potassium–argon and fission-track dating of Libyan Desert Glass, and strontium and neodymium isotope constraints on its source rocks. In: de Michele, V. (Ed.), Silica '96: Proceedings of Meeting on Libyan Desert Glass and Related Desert Events. Pyramids, Milano, pp. 59–73.

Huss, G.R., Lewis, R.S., 1994. Noble gases in presolar diamonds I: Three distinct components and their implications for diamond origins. Meteoritics 29, 791–810.

Huss, G.R., Lewis, R.S., Hemkin, S., 1996. The "normal planetary" noble gas component in primitive chondrites: Compositions, carrier, and metamorphic history. Geochim. Cosmochim. Acta 60, 3311–3340.

Huss, G.R., Meshik, A.P., Smith, J.P., Hohenberg, C.M., 2003. Presolar diamond, silicon carbide, and graphite in carbonaceous chondrites: Implications for thermal processing in the solar nebula. Geochim. Cosmochim. Acta 67, 4823–4848.

Jakubowski, T., Karczemska, A., Kozanecki, M., 2011. Diamonds in ureilites. Meteorites, 3–8.

Jessberger, E.K., 1999. Rocky cometary particulates. Their elemental, isotopic and mineralogical ingredients. Space Sci. Rev. 90, 91–97.

Kagi, H., Sato, S., Akagi, T., Kanda, H., 2007. Generation history of carbonado inferred from photoluminescence spectra. Am. Mineral. 92, 217–224.

Kenkmann, T., Hornemann, U., Stöffler, D., 2005. Experimental shock synthesis of diamonds in a graphite gneiss. Meteorit. Planet. Sci. 40, 1299–1310.

Kerridge, J.F., 1985. Carbon, hydrogen and nitrogen in carbonaceous chondrites – abundances and isotope compositions in bulk samples. Geochim. Cosmochim. Acta 49, 1707–1741.

Koeberl, C., 2000. Confirmation of a meteoritic component in Libyan Desert Glass from osmium-isotopic data. Meteorit. Planet. Sci. 35 (5, Suppl), A89–A90.

Koeberl, C., Masaitis, V.L., Shafranovsky, G.I., Gilmour, I., Langenhorst, F., Schrauder, M., et al., 1997. Diamonds from the Popigai impact structure, Russia. Geology 25, 867–970.

Lewis, R.S., Amari, S., Anders, E., 1994. Interstellar grains in meteorites: II. SiC and its noble gases. Geochim. Cosmochim. Acta 58, 471–494.

Lewis, R.S., Srinivasan, B., Anders, E., 1975. Host phase of a strange xenon component in Allende. Science 190, 1251–1262.

Lodders, K., Osborne, R., 1999. Perspectives on the Comet–Asteroid–Meteorite link. Space Sci. Rev. 90, 289–297.

Longinelli, A., Sighinolfi, G., De Michele, V., Selmo, E., 2011. $\delta^{18}O$ and chemical composition of Libyan Desert Glass, country rocks, and sands: new considerations on target material. Meteorit. Planet. Sci. 46, 218–227.

Ludwig, K., 2000. Isoplot/Ex version 2.2. Berkeley Geochronology Centre Special Publication 1a.

Marty, B., et al., 2008. Helium and neon abundances and compositions in cometary matter. Science 319, 75–78.

Matrajt, G., et al., 2008. Carbon investigation of two Stardust particles: A TEM, NanoSIMS, and XANES study. Meteorit. Planet. Sci. 43, 315–334.

Matrajt, G., Messenger, S., Brownlee, D., Joswiak, D., 2012. Diverse forms of primordial organic matter identified in interplanetary dust particles. Meteorit. Planet. Sci. 47, 525–549.

Mayer, M., 1997. SIMNRA User's Guide. IPP 9/113. Max-Planck-Institut für Plasmaphysik. Garching, Germany. 156 pp.

McKeegan, K.D., Aléon, J., Bradley, J.P., et al., 2006. Isotopic compositions of cometary matter returned by Stardust. Science 314, 1724–1728.

Niedermann, S., 2002. Cosmic-ray-produced noble gases in terrestrial rocks: Dating tools for surface processes. Rev. Mineral. Geochem. 47, 731–784.

Ott, U., 2002. Noble gases in meteorites – Trapped components. Rev. Mineral. Geochem. 47, 71–100.

Ozima, M., Wieler, R., Marty, B., Podosek, F.A., 1998. Comparative studies of solar, Q gases and terrestrial noble gases, and implications on the evolution of the solar nebula. Geochim. Cosmochim. Acta 62, 301–314.

Ozima, M., Zashu, S., Tomura, K., Matshushita, Y., 1991. Constraints from noble-gas contents on the origin of carbonado diamonds. Nature 351, 473–474.

Pepin, R.O., Porcelli, D.P., 2002. Origin of noble gases in the terrestrial planets. Rev. Mineral. Geochem. 47, 191–246.

Petersen, H.I., Rosenberg, P., Nytoft, H.P., 2008. Oxygen groups in coals and alginite-rich kerogen revisited. Int. J. Coal Geol. 74, 93–113.

Podosek, F.A., Honda, M., Ozima, M., 1980. Sedimentary Noble gases. Geochim. Cosmochim. Acta 44, 1875–1884.

Pratesi, G., Viti, C., Cipriani, C., Mellini, M., 2002. Silicate–silicate liquid immiscibility and graphite ribbons in Libyan Desert Glass. Geochim. Cosmochim. Acta 66, 903–911.

Rocchia, R., et al., 1997. The impact origin of Libyan Desert Glass. In: de Michele, V. (Ed.), Silica '96: Proceedings of Meeting on Libyan Desert Glass and Related Desert Events. Pyramids, Milano, pp. 143–149.

Rotundi, A., et al., 2008. Combined micro-Raman, micro-infrared, and field emission scanning electron microscope analyses of comet 81P/Wild 2 particles collected by Stardust. Meteorit. Planet. Sci. 43 (1–2), 367–397.

Rubin, A.E., 2006. Shock, post-shock annealing, and post-annealing shock in ureilites. Meteorit. Planet. Sci. 41, 125–133.

Sandford, S.A., Aléon, J., Alexander, C.M.O.D., et al., 2006. Organics captured from Comet 81P/Wild 2 by the Stardust spacecraft. Science 314, 1720–1724.

Seebaugh, W.R., Strauss, A.M., 1984. A cometary impact model for the source of Libyan Desert glass. J. Non-Cryst. Solids 67, 511–519.

Sharp, Z.D., 2007. Principles of Stable Isotope Geochemistry. Pearson/Prentice Hall, 344 pp.

Sharp, Z.D., Papike, J.J., Durakiewicz, T., 2003. The effect of thermal decarbonation on stable isotope compositions of carbonates. Am. Mineral. 88, 87–92.

Shelkov, D., Verchovsky, A.B., Milledge, H.J., Pillinger, C.T., 1997. Carbonado: A comparison between Brazilian and Ubangui sources with other forms of microcrystalline diamond based on carbon and nitrogen isotopes. Russ. Geol. Geophys. 38, 332–340.

Stadermann, F., et al., 2008. Stardust in stardust; the C, N, and O isotopic compositions of Wild 2 cometary matter in Al foil impacts. Meteorit. Planet. Sci. 43, 299–313.

Trueb, L.F., de Wys, E.C., 1969. Natural poly-crystalline diamond. Science 165, 799–802.

Ward, C.R., Li, Z., Gurba, L.W., 2005. Variations in coal maceral chemistry with rank advance in the German Creek and Moranbah Coal Measures of the Bowen Basin, Australia, using electron microprobe techniques. Int. J. Coal Geol. 63, 117–129.

Wasson, J.T., 2003. Large aerial bursts; an important class of terrestrial accretionary events. Astrobiology 3, 163–179.

Wieler, R., 2002. Noble gases in the Solar System. Rev. Mineral. Geochem. 47, 21–70.

Wieler, R., Anders, E., Baur, H., Lewis, R.S., Signer, P., 1992. Characterization of Q-gases and other noble gas components in the Murchison meteorite. Geochim. Cosmochim. Acta 56, 2907–2921.